

## XAFS at the Pacific Northwest Consortium-Collaborative Access Team undulator beamline

Steve Heald,<sup>a</sup> Edward Stern,<sup>b</sup> Dale Brewe,<sup>b</sup> Robert Gordon,<sup>c</sup> Daryl Crozier,<sup>c</sup> Detong Jiang,<sup>d</sup> and Julie Cross<sup>b</sup>

<sup>a</sup>PNNL, Bldg. 435E, Argonne IL 60439, USA, <sup>b</sup>University of Washington, Seattle WA, USA, <sup>c</sup>Simon Fraser University, Burnaby, Canada, <sup>d</sup>Canadian Light Source, Saskatoon, Canada. Email:heald@aps.anl.gov

The Pacific Northwest Consortium-Collaborative Access Team (PNC-CAT) has begun operating an insertion device beamline at the Advanced Photon Source. The beamline has been extensively used for XAFS studies. This paper summarizes its capabilities, and our initial operational experience. The beamline is based on APS undulator A, and incorporates full undulator scanning. The monochromator is liquid nitrogen cooled and has both Si(111) and Si(311) crystals in a side-by-side configuration. Crystal changes only take a few minutes. The crystals cover the energy range from 3-50 keV with fluxes as high as  $2 \times 10^{13}$  ph/sec. Microbeams can be produced using Kirkpatrick-Baez mirrors (spot size 1-3  $\mu\text{m}$ ) or tapered capillaries (sub- $\mu\text{m}$  spots). When these optics are combined with a 13-element Ge detector, the beamline provides powerful microbeam imaging and spectroscopy capabilities. Experimental examples from the environmental field and *in-situ* UHV film growth will be discussed.

**Keywords:** Undulator beamline, microfocusing, MBE

### 1. Introduction

The Pacific Northwest Consortium-Collaborative Access Team (PNC-CAT) began commissioning an undulator based beamline at the Advanced Photon Source (APS) in 1997. The beamline has recently begun full operations, and will be open to outside users in the summer of 2001. This paper describes the beamline hardware, initial operational experience and experimental capabilities. The beamline is a multipurpose design and can be used for many types

of scattering and imaging experiments in addition to XAFS. However, in this paper we will concentrate on describing the XAFS and micro-XAFS capabilities.

### 2. Beamline Hardware

The beamline has a simple design consisting of a liquid nitrogen cooled, fixed-exit monochromator followed by a toroidal focusing mirror. These supply a beam to two large experimental hutches in series. The first hutch is for general use, supporting a variety of XAFS, imaging and scattering experiments. The second hutch is dedicated to a large 8-circle PSI diffractometer and MBE capabilities. Setup of time consuming surface experiments can occur while experiments are ongoing in the general-purpose hutch. To bring beam to the second hutch, a He filled flight path is installed, and access to the first hutch is restricted.

The most important component for XAFS experiments is the monochromator. The mechanism is based on a design from the BESSRC-CAT (Ramanathan et al. 1995). The vacuum chamber is divided into two sections. The rotation stage is connected to the crystal carriage by a rigid shaft rotating in a close fitting, but non-contacting collar. The small gap (0.1mm) provides sufficient isolation that the relatively dirty rotation stage and encoder can operate at  $10^{-7}$  torr, while the main chamber operates as low as  $10^{-9}$  torr. This allows us to operate without any windows between the monochromator and storage ring. The crystal rotation is provided by a Huber 430 rotation stage, and a Heidenhain ROD 800 encoder provides angular resolution to 1 microradian. Initially, the stepping motor driving the Huber was outside the vacuum, connected via a ferrofluidic rotary feedthrough. The extra shafts and couplings in this arrangement resulted in non-uniform stepping due to excessive windup. While the encoder always records the actual energy, this caused problems when attempting fine steps in edge regions. Currently a microstepping in-vacuum motor is directly coupled to the Huber.

A unique addition to the original design is the mounting of two sets of crystals side-by-side. Both sets are continually cooled, which means crystal change is a simple matter of translating the monochromator by 63 mm horizontally. This can be done in a few minutes. Currently we use Si (111) and Si (311) reflections to cover the energy ranges of 4-27 and 8-50 keV respectively. The undulator provides even higher energies that could be accessed using the Si (333) reflection, but this has not proved necessary to date.

The first crystal design is similar to the one described by Lee et al. (2000) except the nitrogen flow channels are perpendicular to the

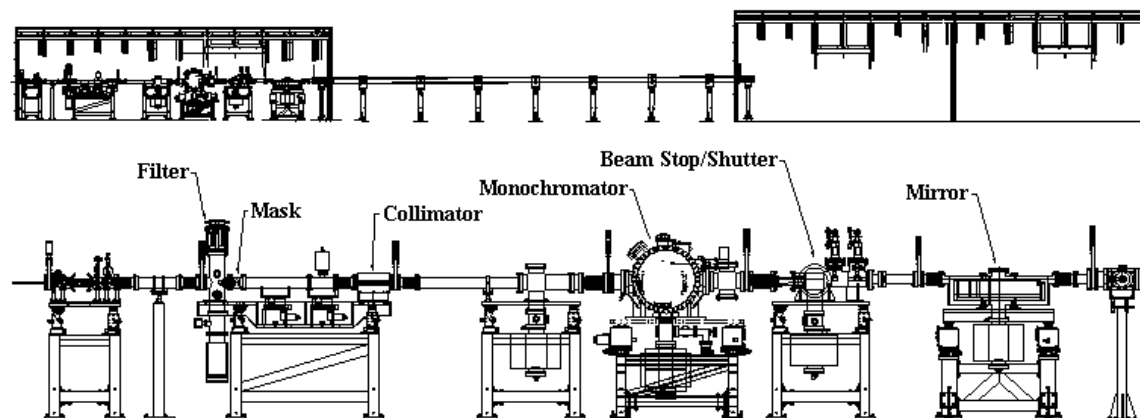


**Figure 1**  
Side view of the undulator beamline, and detailed layout of the optical components for the undulator beamline.

beam direction. The seals are made by indium coated C-rings. In our case, there are three sets of seals: two with the Invar endcap manifolds, and one between the two crystals. This system has proven reliable, and can be thermally cycled several times before the seals need replacement. The second crystal assembly is indirectly cooled through Cu braids. Typical operating temperatures as measured by a thermocouple attached to the Cu crystal mount are between 150-170° K. The surface of the first crystal is expected to operate in the range of 85-110° K for the various undulator gap settings. The Si lattice parameter has a minimum near 125° K. Therefore, the lattice parameters of the first and second crystals are quite similar, and there is very little vertical motion of the beam due to dispersion as the energy is changed. The largest component of vertical beam motion is due to crystal detuning to minimize harmonics. The amount of detuning needed depends on energy. This results in about a 1 mm vertical motion of the beam from low energies to high energies. When a mirror is used to reduce harmonics, this vertical motion can be eliminated.

Harmonic reduction and focusing can be accomplished with the toroidal mirror that follows the monochromator. This mirror has been installed and has been operated in the unbent configuration. The bender motor will be installed soon. The unbent mirror seems to be close to specifications and when bent should provide a spot size of about 300  $\mu\text{m}$ . It is positioned in a slightly demagnifying condition, reducing the beam size by 1.3-1.7 times depending on the experiment position. The mirror is made of fused silica, and is coated with three different metal stripes, Rh, Pt, and Al. The central stripe is Rh, and it provides the best focus. It can operate in the region between its L and K edges (3.5-23 keV). The other two stripes are located 6 mm on either side of the centerline, and will be used to extend the energy range to 30 keV (Pt) or for harmonic rejection at energies below 8 keV (Al). Because they are off the bending axis, the focus will be degraded somewhat for the side stripes. Raytracing indicates the degradation is mainly in the horizontal focal spot size, which increases by about a factor of two. For certain microfocusing optics and energies above 30 keV, it is necessary to drop the toroidal mirror out of the beam. The beam pipe and Be window following the mirror are large enough to accommodate the resulting beam motion (up to 100 mm) without the movement of any beamline components.

### 3. Microfocusing

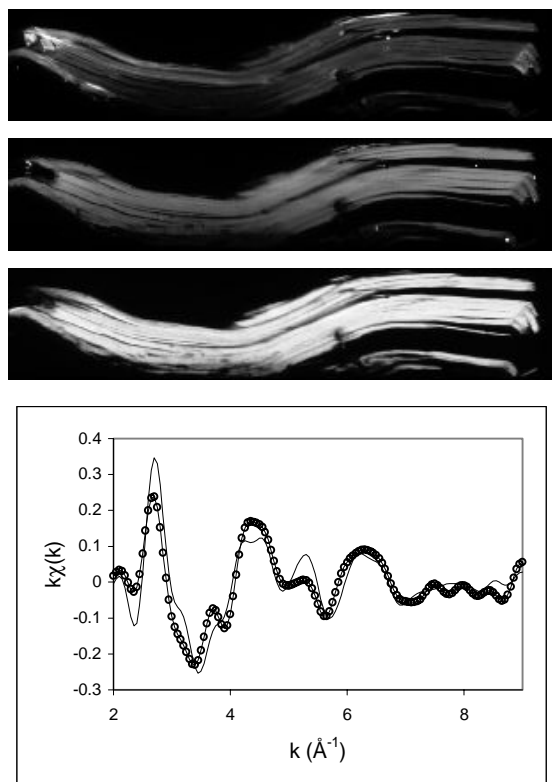
Currently two types of microfocusing optics are employed: Kirkpatrick-Baez (K-B) mirrors and tapered capillary concentrating optics. The K-B mirrors are based on a design from the CARS-CAT (Yang et al. 1995). Two sets are available with mirrors 100 mm and 200 mm long respectively. The 100 mm set provides a focus down to 1  $\mu\text{m}$  at energies up to 18 keV. Typical flux is approximately  $1 \times 10^{11}$  ph./sec. This set has also been used up to 25 keV with a focus size of about 2  $\mu\text{m}$ . It is the main optic used for microspectroscopy since it provides a smooth energy transmission curve and provides a working distance of 30 mm from the end of the mirror. The long mirror system is similar except it collects 4x the flux, has a larger working distance (150 mm), and focuses to 3  $\mu\text{m}$ . It is used for experiments that do not require the best resolution, or in conjunction with the toroidal mirror as described below.

Figure 2 shows some examples of data taken with the short K-B mirrors and a 13-element Ge detector. The sample is a cross-sectional slice of a mica flake from the Hanford site, and is part of a study to understand the interaction of environmental Cs with typical Hanford site minerals. Simultaneous elemental images with 1  $\mu\text{m}$  resolution were taken for six different elements using the energy resolution of the Ge detector. Three examples are shown in the figure. XAFS spectra were then taken for Cs, Ti, Ba, Mn, and Fe in

low and high Cs locations. Most of the spectra were similar in the two regions. The biggest difference was seen for the Mn data as shown in Figure 2. Analysis is underway to understand the structural changes that enhance Cs absorption.

The short mirror must be used without the toroidal mirror to provide the minimum focal spot size. Since the entrance aperture of the mirrors is about 0.3 x 0.3 mm, a significant fraction of the monochromator output (approximately 1 x 3 mm) is not used. For experiments that do not require the smallest focus, the K-B mirrors can be combined with the toroidal mirror. In this case, the toroidal mirror is set to focus a few meters past K-B mirrors, which intercept the beam and direct it to a new focal point closer to the mirrors. For example, if the original focus is 5 m past the K-B mirrors, and the mirrors are focusing to 1 m, the beam size is further reduced by a factor of 5 from the toroidal mirror focus. This can reduce the focus to below 100  $\mu\text{m}$ ; a size well matched to experiments such as glancing angle XAFS. In this configuration, the beam size at the K-B mirror entrance has been reduced by the toroidal mirror, and the long K-B mirrors can collect essentially the entire undulator beam.

The tapered capillaries (Heald et al., 1996) have been used to provide sub-micron beams. Capillaries with outlet sizes of 0.5 and 0.7  $\mu\text{m}$  have been tested. Other groups have reported spot sizes as small as 0.1 micron (Hoffman et al. 1994). The entrance aperture of these capillaries is about 150  $\mu\text{m}$ . The capillaries have two disadvantages for spectroscopy. The working distance is small (typically 50-100  $\mu\text{m}$ ), which prevents the use of an  $I_0$  detector



**Figure 2**

Top images: cross-sectional views of the Cs (top), Mn (middle) and K (bottom) concentrations in a biotite mica flake after exposure to a dilute solution of Cs. The image size is 780 x 170  $\mu\text{m}$ . The Cs typically accumulates in weathered regions near the edge. Bottom: XAFS for the Mn edge in the high (points) and low (line) Cs regions.

between the capillary outlet and sample. Also, the transmission function has some energy dependent structure. This structure is reproducible, and with careful calibration can be removed for concentrated samples (Heald et al. 1996), but often will cause artefacts for dilute samples. The structure is smooth enough, however, that near edge studies are generally possible.

## 4. MBE-UHV studies

The first of two systems for molecular beam epitaxy and *in-situ* X-ray studies of thin metal films has become operational at the PNC-CAT beamline. This system, MBE1, is constructed around a custom Thermionics GB-16 Manipulator that permits sample orientation for *in-situ* preparation and polarisation-dependent X-ray studies involving XAFS, reflectivity and X-ray standing wave techniques. A table upgrade is under construction that will make the MBE1 system compatible with the toroidal mirror on the insertion device line and more readily transferable to the bending magnet line. The second system, MBE2, is awaiting construction and will combine surface diffraction with many of the capabilities of MBE1.

The first experiments performed in MBE1 involved examining the structure of iron films on the (4x6) reconstructed (001) surface of gallium arsenide. The small (1.4%) mismatch between the body-centred cubic iron lattice and half the GaAs lattice constant facilitated the growth of high-quality films with thickness between 3 and 15 monolayers (ML) of Fe. The polarisation-dependent positioning capabilities in MBE1 allowed the in-plane and out-of-plane Fe lattice constants to be determined by glancing-angle XAFS, an example of which is shown for 9.3ML of Fe in Figure 3. Analysis (Gordon et al., 2000) has indicated a tetragonal distortion of the iron film with  $c/a = 1.03(1)$ . A detailed analysis of the thickness dependence of this distortion, which will have an impact on the interpretation of the magnetic anisotropy in these films (Monchesky et al., 1999, Gordon et al., 2000) is underway.

## 5. Other endstation equipment

The beamline is equipped with a full range of equipment to support experiments in the endstations. A full complement of detectors is available including ion chambers for transmission and fluorescence, and a 13-element Ge detector with digital electronics. Low temperature experiments can be accommodated using a top-loading closed-cycle refrigerator that operates from 12-300 K.

Time-resolved experiments will be supported with a high repetition-rate Ti-sapphire mode-locked laser. This laser is specially designed to allow operation up to the storage ring revolution rate. This allows it to be synchronised with a single bunch, making efficient use of the available X-rays. Based on experience at other APS beamlines, we expect that pump-probe experiments can be conducted with better than 1 nsec time resolution. The high repetition-rate dictates that the energy per pulse is a few microjoules. However, by focusing the laser beam to a few microns, adequate intensity can be obtained to excite or even melt many samples. We have already demonstrated that the x-ray beam can be focused to similar dimensions. First experiments with the laser are expected in 2001.

Diffraction anomalous fine structure (DAFS) experiments are supported by a small kappa-geometry diffractometer or by a large 8-circle psi-geometry instrument. Both of these are currently being commissioned, and should be fully operational in 2001 also.

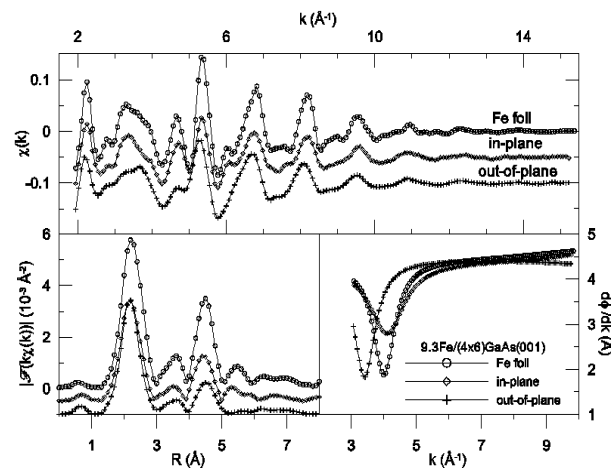


**Figure 3**  
Fe K-edge fluorescence XAFS interference functions, k-weighted Fourier transform magnitudes and beating analysis (derivatives of phase of the inverse transform of the first peak) for 9.3ML of Fe on (4x6) reconstructed GaAs(001) examined *in-situ* with the X-ray polarisation in and out of the plane of the substrate. Transmission data for Fe foil are also shown for comparison.

Finally, a diamond phase plate can be used to control the x-ray polarisation. It operates up to 12 keV, and has been used to provide a vertically polarised beam, as well as circular polarisation for MCD studies. Work is proceeding on developing crystals to extend the upper energy range.

The PNC-CAT project is supported by funding from the U.S. Department of Energy Basic Energy Sciences, the National Science Foundation, the University of Washington, the Natural Sciences and Engineering Research Council in Canada, and Simon Fraser University. The Pacific Northwest National Laboratory is operated by Battelle Memorial Institute for the U.S. DOE. The APS is supported by the U.S. DOE BES, Office of Energy Research, under Contract No. W-31-109-Eng-38.

## References

- Gordon, R. A., Crozier, E. D., Jiang, D. T., Monchesky, T. L., and Heinrich, B. (2000), Phys. Rev. B 62, 2151-2157.
- Heald, S. M., Brewster, D. L., Kim, K. H., Brown, F. C., Barg, B., and Stern E. A. (1996), Proc. SPIE 2856, 36-47.
- Hoffman, S. A., Thiel, D. J., and Bilderback, D. H. (1994), Opt. Eng. 33, 303-306.
- Lee W.-K., Fernandez P. and Mills D. M. (2000) J. Synchrotron Rad. 7, 12-17.
- Monchesky, T. L., Heinrich, B., Urban, R., Myrtle, K., Klaua, M., and Kirschner, J. (1999), Phys. Rev. B 60, 10242-10251.
- Ramanathan, M., Beno, M.A., Knapp, G. S., Jennings, G., Cowan, P.L., and Montano P.A. (1995), Rev. Sci. Instr. 66, 2191-2194.
- Yang, B. X., Rivers, M., Schildkamp, W., Eng, P. J. (1995), Rev. Sci. Instr. 66, 2278-2280.